PERGAMON

Building and Environment 36 (2001) 167–180

BUILDING AND ENVIRONMENT

www.elsevier.com/locate/buildenv

Buoyancy-driven flow through a stairwell

A.A. Peppes*, M. Santamouris, D.N. Asimakopoulos

Department of Physics, Division of Applied Physics, University of Athens, Building PHYS-V, Group Buildings Environmental Studies, GR-157 84, Athens, Greece

Received 1 April 1999; received in revised form 23 August 1999; accepted 22 October 1999

Abstract

The present work concerns the measurement and the computational fluid dynamics (CFD) modeling of buoyancy-driven air flow through a stairwell that connects the two individual floors of a residential building. A series of experiments was performed in order to study the mass and heat transfer between the two floors. Air flow rates through this stairwell were measured using a single tracer gas decay technique. The analysis of results provided relations which can predict the mass and heat flow rate as a function of the interzone average temperature difference. These results were compared with values estimated by using validated CFD algorithms and showed very good agreement. © 2000 Elsevier Science Ltd. All rights reserved.

1. Introduction

The study of energy and mass transfer between different zones in buildings has attracted increasing international interest and research effort. This issue is of great importance due to its impact on energy conservation, thermal comfort, control of contaminants and spread of smoke in the interior of buildings. Airflow through vertical openings has been widely researched. However, little work has been done on the air flow through horizontal openings, such as stairwells and ventilation shafts, especially those concerning buoyancy-driven flows. Indeed, very few authors have studied these phenomena and limited systematic experimental data is available in the literature.

A limited number of studies related to these phenomena have been reported. Brown [1] has investigated the buoyancy-driven vertical air flow through small rectangular openings of various sizes in horizontal partitions. The results are expressed in terms of a relation of a ratio of Nusselt to Prandtl number as an increasing function of the Grashof number.

Epstein [2] has also performed an experimental investigation on buoyancy-driven exchange vertical flows. Experiments were carried out in a small two-compartment apparatus in which a density-driven exchange flow occurred by using brine above the horizontal partition and fresh water below the partition. The measurements covered a wide range of opening sizes. Epstein defined four different flow regimes in order to extend and classify the findings of previous studies. He also fitted his results to the relation of a dimensionless Froude number in terms of the thickness of the partition separating the two compartments to diameter ratios of the openings. Both of these studies dealt with purely buoyancy-driven flows and made no allowance for the net flow to affect the process.

Klobut and Siren [3] have explored the influence of several parameters on combined forced and density-driven air flow through large openings of two different sizes, located in the horizontal partition of a two-compartment apparatus. Their research effort focused on the derivation of a mathematical model of the phenomenon with the combined effect of the temperature difference and the forced net flow.

Reynolds [4] and Zohrabian et al. [5] have conducted experiments in a reduced scale model of a typical stairwell. They investigated the air flow through an inclined channel connecting the two compartments of the model. The flow was driven by energy input from

* Corresponding author.

PII: S0360-1323(99)00062-1

Nomenclature

A	effective cross-sectional area of the opening connecting the two zones (m^2)
C	coefficient of discharge (dimensionless)
C_1	concentration of the tracer gas at time t in zone 1 (ppm)
C_2	concentration of the tracer gas at time t in zone 2 (ppm)
c_p	specific heat of air (J kg^{-1} K^{-1})
Gr_H	Grashof number, ($\beta\ g\ \Delta T\ H^3\ /\nu^2$) (dimensionless)
g	acceleration due to gravity (m s^{-2})
H	thickness of the floor separating the two zones (m)
I	infiltration rate (m^3 s^{-1})
M	mass flow rate (kg s^{-1})
Q	volumetric flow rate (m^3 s^{-1})
$\mathbf{Q}$	heat flow rate (J s^{-1})
t	time (s)
T	mean absolute temperature of the two zones (K)
V_1	effective volume of zone 1 (m^3)
V_2	effective volume of zone 2 (m^3)
W	vertical component of air velocity (m s^{-1})

Greek symbols

β	coefficient of thermal expansion (K^{-1})
ΔT	average air temperature difference between the two zones (°C)
ν	kinematic viscocity (m^2 s^{-1})
ρ	average air density (kg m^{-3})

an electric panel heater located in the lower zone of the model. Mass and heat flow rates were estimated from the measurements of air temperature and air velocity at various cross-sections of the model. In these experiments a through-flow was observed. This flow was caused naturally by providing openings in both compartments and not mechanically by fans. Reynolds [4] and Reynolds and Mokhtarzadeh-Dehghan [6], have also extracted a mathematical model for the phenomenon by applying dimensional analysis. A relation between the Froude number and a ratio of the temperature difference to mean temperature, corrected by a function of the Reynolds number, is proposed. Further experimental investigation was suggested to discover whether this function varies markedly from one stairwell type to the next, and possibly to develop a body of empirical data characterizing the more common stairwell forms.

Riffat [7] has studied the energy and mass transfer between the two floors of a full-scale conventional house. Actually, the investigation dealt with the air flow through a doorway separating one space on the lower floor from the rest of the same floor and the upper floor. Air flow rates between the two floors were measured using a single tracer gas technique, and the temperatures at various points in each floor were measured using thermocouples. The mass flow rate and the coefficient of discharge for the doorway were found to be functions of the temperature difference between the two floors.

The above studies have mainly been of experimental or analytical nature. Related to buildings in general, there are numerous publications available on computation of air flow in rooms or cavities, but similarly very few studies have been concerned with the application of computational fluid dynamics (CFD) to air flow in horizontal openings and stairwells. Zohrabian et al. [5] used their own finite-volume program to predict the two-dimensional buoyancy-driven flow in a stairwell model. Ergin-Ozkan et al. [8] have conducted a similar numerical study of three-dimensional buoyancy-driven flow in a stairwell and compared predictions with experimental data.

Riffat and Shao [9] have also performed a study concerned with CFD modeling of natural convection through a horizontal opening between two zones. A simplified geometry was chosen for the numerical analysis of only one case, due to the lack of information regarding boundary conditions. Comparison of the predicted air flow rate and that based on experimental measurement showed good agreement, with a relative difference of 10.5%.

Vertical air movement occurring in stairwells is one of the most important mechanisms of interzone transfer in the interior of buildings. Thermal buoyancy is one of the factors that induces such flow processes, especially in naturally ventilated buildings. The importance of the temperature effect on these phenomena has been indicated in studies performed in a multi-storey real building [10] as well as in two-storey dwellings [7,11]. Tracer gas measurement techniques and recent research in CFD allow scope for conducting measurements and extensive modeling to investigate these phenomena. The objectives of this work are to study the buoyancy-driven air movement through a typical stairwell that connects the two floors of a full-scale building, to compute the heat and mass transfer between the interconnected floors, to analyze this situation using CFD algorithms and finally, via comparison of the predicted and measured values, to consequently improve the existing predictive methods of such processes.

2. Experimental Set-up

2.1. Experimental procedure and instrumentation

Experimental studies were performed in a two-storey, naturally ventilated, residential building located in a rather densely built-up area in the western suburbs of Athens. Most of the neighboring buildings are also residential and have between two- and four-storeys. The intention of these studies was to investigate the buoyancy-driven air flow through a stairwell that connects the floors of the building. The specific stairwell geometry is common in this type of building. The stairwell extends to a height of 6.3 m, while the lower and upper floor have an effective volume of 29.1 and 35.8 m^3, respectively. Each floor is 3.0 m high. Fig. 1 shows a schematic diagram of this building with the main dimensions and the locations of the instruments.

Air flow measurements were carried out using a single tracer gas decay technique. Several tracer gases are available, but N_20 was chosen for this work since it has desirable characteristics in terms of detectability, safety and cost and it has been used successfully in previous air movement studies. The concentration of gas was measured using an infrared gas analyzer (accuracy: ±1%). The sampling period was set at 25 s. The following experimental procedure was implemented. At the beginning of each experiment the opening between the two floors was closed by a PVC sheet and every gap between this sheet and the adjacent wall surfaces was sealed. In addition, all the openings, such as the entrance door, the doors connecting the stairwell with the apartments and the windows were kept closed and sealed during all the experiments. Therefore, the selected two zones were isolated from the rest of the building. Some small openings and cracks were also sealed in order to reduce the infiltration as much as possible. Tracer gas was released in the lower floor, where it was mixed with air. The mixing process was accelerated using small fans near the injection points of gas. After uniformity had been achieved in the lower floor, the PVC sheet was removed and the evolution of tracer gas concentration in both floors, was then monitored. According to this technique, the two floors were considered to represent two different zones. Hereafter, the lower floor will be designated zone 1 and the upper floor zone 2. Six sampling points, three in each floor, were carefully chosen and distributed so as to measure the concentration variation with time at various locations of the experimental space (Fig. 1). Since a single tracer gas and one analyzer was used, only one concentration reading in each zone was obtained at the actual sampling time. The sequential sampling of the gas concentration resulted in a time lag between measurements. It must be noted that the decay technique applied requires that the concentrations in the two floors are recorded simultaneously. In order to reconstruct the missing concentrations, the simplest method of linear interpolation was adopted. The same method has been applied successfully in other studies [12]. Furthermore, the mean concentration level for each zone was calculated as the mean value of the three measuring points placed in this zone, assuming that these measurements corresponded to the same time. At any rate, insignificant spatial variations in either zone concentration for any sampling period, were identified.

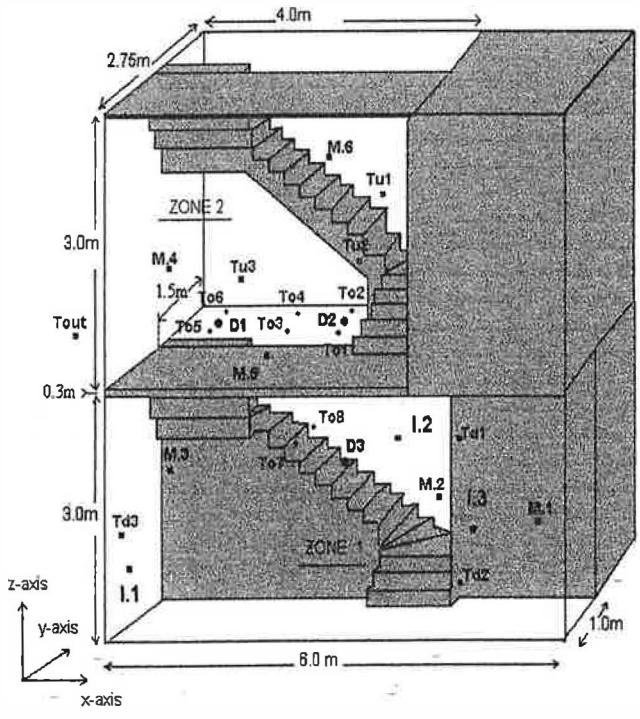

Fig. 1. Schematic diagram of the stairwell and locations of the instruments; T, temperature sensor; D, air velocity sensor; M, measuring point; and I, injection point.

The thermal performance of the stairwell was constantly monitored. The air temperature was recorded by thirteen temperature sensors (accuracy ±0.2°C) which had already been calibrated. The time interval between successive measurements was set at 30 s. The location of these sensors in each zone is important if the heat flow between the zones is to be measured accurately. In the present work air temperature sensors were placed at various locations and heights in each zone, in order to derive the average air temperature of each zone and simultaneously, to reveal possible thermal stratification (Fig. 1). The mean air temperature for each floor was calculated as the mean value of the temperatures provided by the corresponding sensors placed in this floor. In addition, a number of such sensors were placed across the horizontal opening separating the two zones, so as to monitor the temperature distribution and its variation with time in that particu-

lar area (Fig. 1). Surface temperatures on almost all the internal surfaces (walls, stairs) were measured by an infrared thermometer (accuracy: ±0.1%). It must be noted that the surface temperatures did not change significantly during each experiment. Limited air velocity measurements were also provided by three air velocity sensors (accuracy ±0.01 m s^{-1}) located in three specific points of the stairwell for all the experiments (Fig. 1). The outside air temperature and the wind speed during the measurement period were also recorded. Finally, the flow was visualized using smoke injected at various points in the stairwell.

2.2. Flow calculation

Since air can infiltrate from outside the building into each zone (Q_{01} and Q_{02}) and exfiltrate from each zone to the outside (Q_{10} and Q_{20}), some tracer gas is transported to the outside. Simultaneously, since air can be exchanged between the two zones through the stairwell in both directions (Q_{12} and Q_{21}), some tracer gas will be carried into zone 2 where it mixes with air and some will return to zone 1. Applying the mass balance of the tracer gas in each zone and assuming that both a steady state exists and that the concentration of tracer gas in the outside air is negligible, then the rate of change of tracer concentration in zone 1 and in zone 2 at time t are given, respectively, by:

$$V_1 dC_1/dt = -C_1(Q_{10} + Q_{12}) + C_2 Q_{21} \quad (1)$$

$$V_2 dC_2/dt = C_1 Q_{12} - C_2(Q_{21} + Q_{20}) \quad (2)$$

C_1 is the concentration of the tracer at time t in zone 1 and, similarly, C_2 is the concentration of the tracer at time t in zone 2. The other two volumetric flow rates can be determined using the continuity equations:

$$Q_{01} = Q_{10} + Q_{12} - Q_{21} \quad (3)$$

$$Q_{02} = Q_{20} + Q_{21} - Q_{12} \quad (4)$$

These volumetric-balance equations can be solved using the theoretical technique based on the Sinden [13] method. A similar method was adopted by Afonso and Maldonado [14]. According to this method, a multizone system may be represented by a series of cells of known and constant volume that are all connected to a cell of infinitely large volume (outside). Since the unknown flow rates involved in these equations are six, it was suggested by Sinden that Eqs. (1) and (2) could be integrated from two different intervals from the concentration decay curves for each zone. This technique would yield the necessary number of equations to solve for all the unknowns. The equations were integrated using Simpson's rule and the final system of simultaneous equations was solved numerically by Gauss elimination. This method was employed in the present work. It must be noted that this method results to significant errors when it is applied in buildings with more than two zones. Under these situations multiple tracer-gas procedures are recommended [15].

3. Measurements, results and discussion

The air flow rate between the floors is mainly determined by the size and geometry of the opening separating the two floors. This horizontal opening is defined by the stairwell geometry. Furthermore, an additional obstacle was placed suitably across the opening of the first stairwell, decreasing its size. Under this modified configuration, several experiments were performed in order to study the dependence of air flow on the size of opening. Hereafter, the experiments characterized by the original configuration, will be referred to as runs with opening A, while the others will be referred to as runs with opening B. Opening A had horizontal dimensions, taking a plan view of the space, of 2.7 m (x-axis) by 1.5 m (y-axis) while opening B had horizontal dimensions of 2.15 m (x-axis) by 1.5 m (y-axis). Figure 2 shows the schematic diagrams of these two opening configurations.

According to the adopted procedure, the whole experimental space was isolated from the rest of the building and surroundings as much as possible. As a result the interzone air flow studied in the present work was mainly induced by the air temperature difference between the two floors. In general, the air flow rate between the floors is also affected by the temperature difference of these zones. This temperature difference is defined as the difference of the average temperatures of the two zones. In order to investigate the dependence of air flow on the interzone temperature difference, the lower zone was heated, while the upper floor was unheated. This was done by using thermostatically controlled heaters. These heaters were switched on a long time before the beginning of each test to enable the heaters and air in the lower zone to reach thermal equilibrium. It must be noted that the lower zone was isolated from the upper zone prior to the beginning of each run as described in the previous section. In some experiments these heaters were switched off in order to achieve a very low temperature difference (near isothermal conditions) between the two zones.

Eleven experiments were carried out in this building, under a variety of temperature differences between the two zones and for both opening configurations described before. In addition, some preliminary experiments were also performed under various climatic conditions, in order to estimate the infiltration/exfiltra-

tion rate characterizing the whole space. This infiltration was caused by the temperature difference between the inside and outside of the building and the wind speed. In these experiments tracer gas was released in both zones via three injection points placed in specific locations. The opening connecting the two floors, remained open for the whole duration of these experiments. When the mixing was satisfactory in both zones, the injection stopped and concentration at every measuring point was constantly monitored throughout each of these experiments. The tracer decay method was adopted for the estimation of the infiltration rate. According to this method, the decrease of the tracer gas concentration is given by the following equation:

$$C(t) = C(t_0)\exp(-It) \tag{5}$$

where $C(t)$ and $C(t_0)$ are the tracer gas concentration at time t and $t = 0$, respectively. Also, I is the infiltration rate. The air changes per hour have been calculated for each sampling point and then the mean value for the whole experimental space was calculated as the mean of all sampling points. The infiltration rate was found to range below 0.0063 $m^3\ s^{-1}$ for all these experiments. This result verified the initial consideration that the infiltration rate would not significantly affect the interzone air flow rate through the stairwell. Nevertheless, the flow induced by the infiltration/exfiltration during each run, was subtracted from the total air flow between the two floors in order to get more accurate results.

The analysis of the experimental data verified that the application of the method based on the mass balance of the tracer gas for the calculation of air flow rate between the floors was valid. Indeed, a steady state existed since the climatic conditions remained almost constant for the whole duration of each experiment. Table 1 shows the experimental conditions during these experiments. In particular, it shows the outside temperature and the wind speed for the various runs. Furthermore, each floor was characterized by homogeneity as concerns the concentration level and the air temperature. The relative difference between the concentration

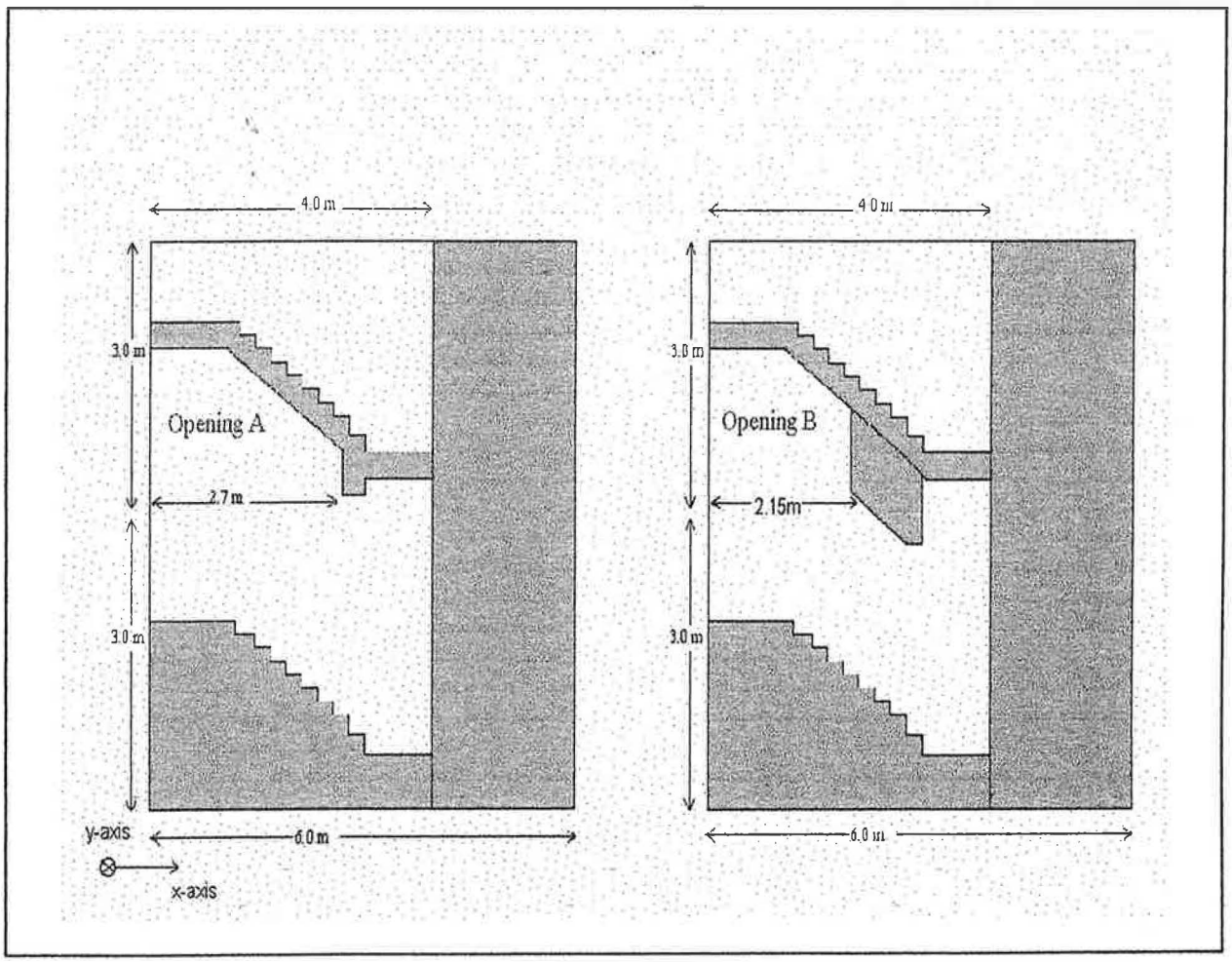

Fig. 2. Schematic diagrams of the two opening configurations.

Table 1
Experimental conditions

Experiment	Outside temperature (°C)	Wind speed (m/s)
1	14.8	1.8
2	15.6	1.6
3	16.7	1.5
4	17.5	1.4
5	17.5	1.3
6	19.5	1.4
7	19.6	1.7
8	18.1	1.3
9	19.6	1.7
10	20.4	1.2
11	20.0	1.3

recorded at various measuring points and the mean concentration level of each floor remained below 6% for almost all time steps. Similarly, the absolute value of the difference between the air temperature measured by temperature sensors located at various points and the mean air temperature of each floor remained below 0.6°C for almost all measurements. These findings verified the initial consideration of the two zones.

The air flow volumetric rates between the two zones were calculated from tracer gas concentration data using the method described previously. Fig. 3 shows the air temperature in zones 1 and 2 against time during the eleventh experiment. The average temperature difference was 2.7°C. This Figure indicates that the values of the zone temperatures did not change significantly during this experiment. The volumetric air flow rate between the two zones was found to be 0.101 $m^3\ s^{-1}$. Fig. 4 shows tracer gas concentration against time during the second experiment, where the temperature difference was 0.5°C. The volumetric air flow rate between the two zones was found to be 0.070 $m^3\ s^{-1}$. In general, experiments were carried out for average temperature differences between 0.2 and 6.2°C and the corresponding volumetric air flow rates between the two zones were found to range between 0.039 and 0.170 $m^3\ s^{-1}$. Table 2 shows the average temperature differences between the zones and the calculated volumetric flow rates for the various runs. The results indicate that the volumetric air flow rate increased when the temperature difference increased. Furthermore, this rate was found to be higher for the greater size of opening A. These results verified that the air flow rate through the stairwell is a function of the temperature difference between them and the size of the opening.

The theoretical analysis for the air flow rate through an opening in horizontal partition separating two zones, has been carried out by previous researchers [1,9]. According to this analysis, assuming that the flow of air is one dimensional and the viscous effect is negligible, Bernoulli's equation yields that volumetric air flow rate can be given approximately by:

$$Q = AC\sqrt{\Delta TgH/T} \tag{6}$$

In addition, the mass and the heat flow rate can be given respectively, by:

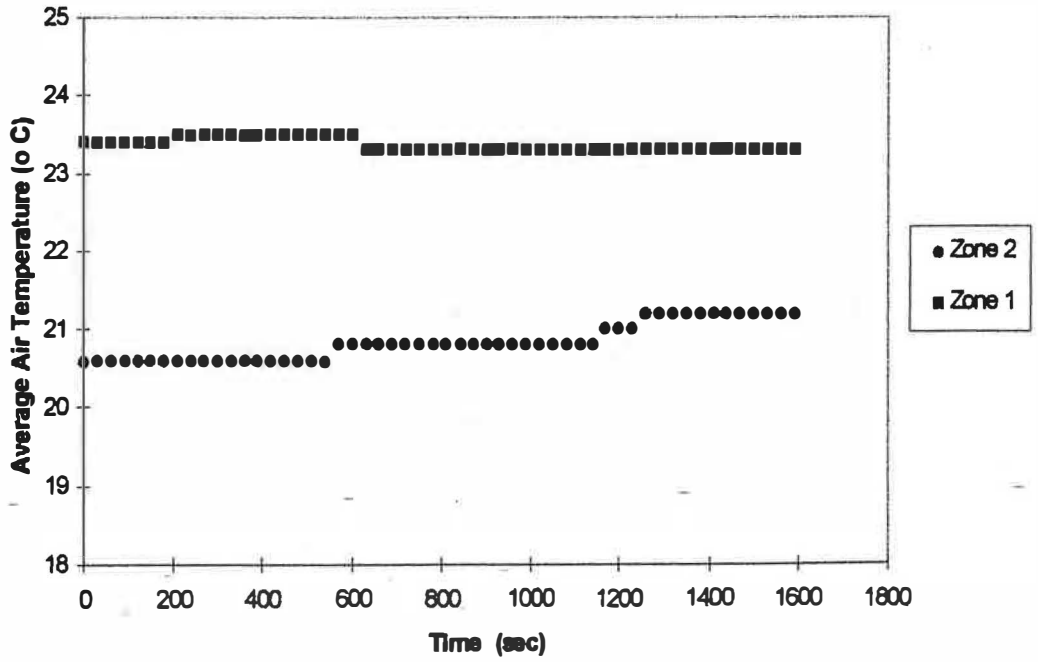

Fig. 3. Variation of air temperature with time during the 11th experiment.

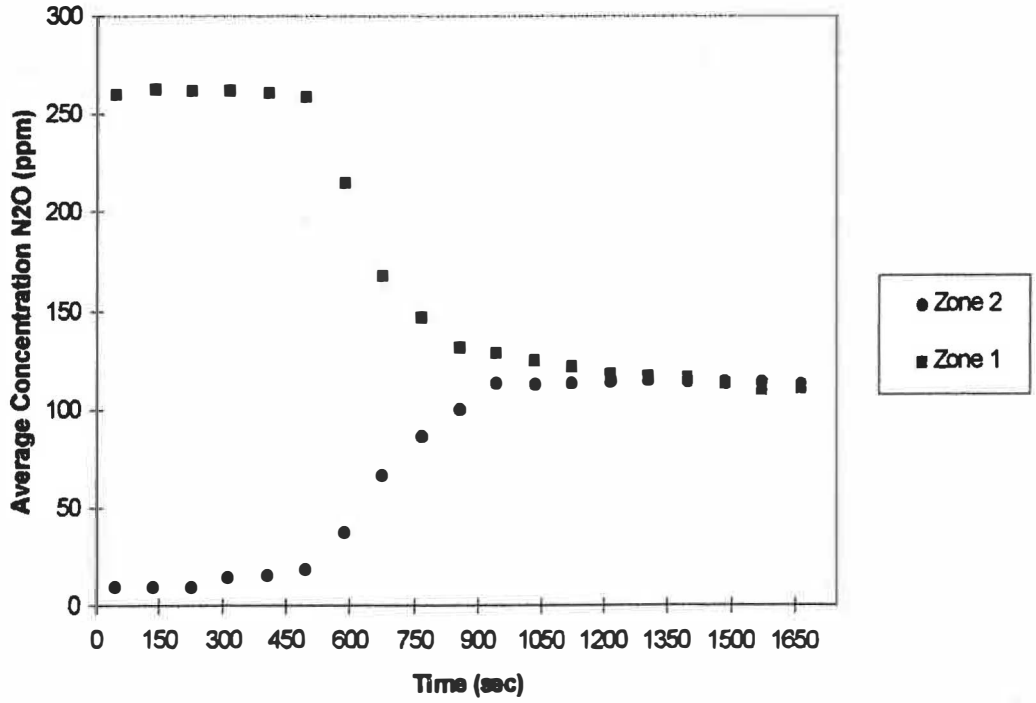

Fig. 4. Variation of N_2O concentration with time during the second experiment.

$$M = \rho A C \sqrt{\Delta T g H / T} \tag{7}$$

$$\mathbf{Q} = \rho c_p A C \sqrt{gH} (\Delta T)^{1.5} / (T)^{0.5} \tag{8}$$

In these equations, H is the thickness of the floor separating the zones. These equations were adopted despite the complex geometry of the specific configuration. It must be noted that the characteristic dimensions of the horizontal opening of this study cannot be easily determined. In fact, this opening was formed by the specific stairwell geometry. For instance, although the floor separating the two zones appeared at only one side of the opening (Fig. 1), the thickness of this floor was accepted as the effective thickness (H) for the air flow, which is involved in the equations presented. This thickness was 0.3 m. In addition, the exchange of air within the opening in the horizontal direction was considered to be negligible. The flow visualization tests and the simulations carried out at the next stage of this study verified this consideration.

Eq. (6) yields the theoretical value of the volumetric flow rate between the two zones. To evaluate the coefficient of discharge for this opening, the measured air flow rate was divided by the corresponding flow given by Eq. (6) for $C = 1$. Fig. 5 shows the variation of the coefficient of discharge with the ratio $\Delta T/T$. It was found that the coefficient of discharge was rather independent of the opening size. It was also found to decrease from about 0.76 to 0.34 as the temperature

Table 2
Results

Run	Opening configuration	Average temperature difference between zones 1 and 2 (°C)	Volumetric flow rate between zones 1 and 2 (m^3/s)
1	Opening A	6.2	0.170
2	Opening A	0.5	0.070
3	Opening A	0.2	0.060
4	Opening A	3.3	0.130
5	Opening A	1.1	0.094
6	Opening B	4.9	0.121
7	Opening B	3.4	0.104
8	Opening B	0.7	0.060
9	Opening B	2.4	0.099
10	Opening B	0.1	0.039
11	Opening B	2.7	0.101

difference between the two floors increased from 0.2 to 6.2°C (Fig. 5). This decrease in the coefficient of discharge may be due to an increase in interfacial mixing as a result of the direct transfer of some cold air from the upper zone into the inflowing warm air from the lower zone. Furthermore, the increase in density difference can increase the turbulence in the two zones, which may affect the value of the discharge coefficient. The coefficient of discharge C and the ratio $\Delta T/T$ were correlated very well with r^2 value equal to 0.96. This relation can be given by:

$$C = 0.1469(\Delta T/T)^{-0.2} \tag{9}$$

Neglecting the runs characterized by near isothermal conditions (low temperature difference), the coefficient of discharge was found to be in the range of 0.48 to 0.34. It also appeared to stabilize near 0.34 for high temperature differences. Brown [1] and Riffat [7] investigated similar phenomena and suggested comparable values for this coefficient. The mean velocity of air through the opening of the stairwell was calculated by dividing the measured volumetric air flow rate by the area of this opening. The mean velocities varied between 0.012 and 0.042 m s^{-1}. The air velocities provided by the limited measurements described above, ranged from 0.03 to 0.22 m s^{-1} depending on the temperature difference between the zones and on the location of measurement. From Eqs. (6) and (9), the volumetric air flow rate between the two zones can be given by:

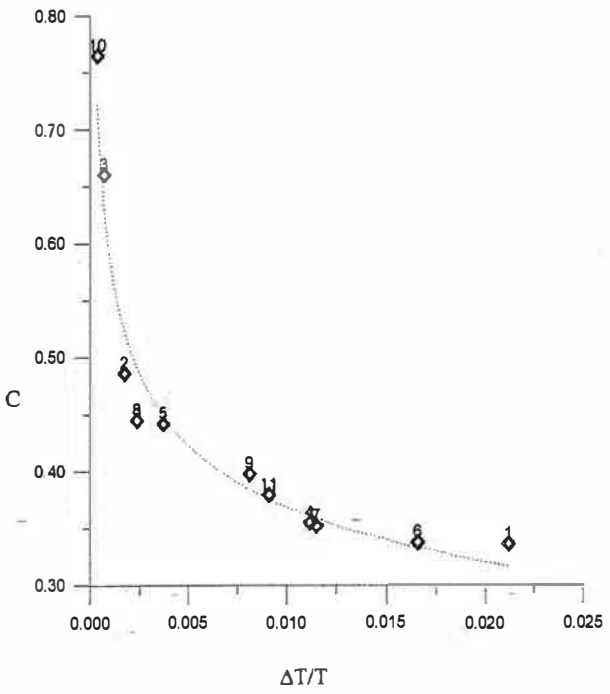

Fig. 5. Variation of coefficient of discharge C with the ratio $\Delta T/T$ (◇: run, – – –: Eq. (9)).

$$Q = 0.1469A\sqrt{gH}(\Delta T/T)^{0.3} \tag{10}$$

This equation indicates that the volumetric flow rate increased linearly with $(\Delta T/T)^{0.3}$ for each opening configuration. Similarly, from Eqs. (7)–(9) the mass and the heat flow rate through the stairwell can be given by the following two equations, respectively:

$$M = 0.1469\rho A\sqrt{gH}(\Delta T/T)^{0.3} \tag{11}$$

$$\mathbf{Q} = 0.1469\rho c_p A\sqrt{gH}(\Delta T)^{1.3}/T^{0.3} \tag{12}$$

A plot of the mass flow rate against $(\Delta T/T)^{0.3}$ for both opening sizes of the stairwell is shown in Fig. 6. The mass flow rate increased linearly with $(\Delta T/T)^{0.3}$ for both opening configurations. Furthermore, the heat flow rate between the two zones was found to be significant.

Alternative formulation may be used to determine the coefficient of discharge and subsequently, the mass and heat transfer through the equations described above. According to this approach, the coefficient of discharge was found to be dependent on the dimensionless Grashof number based on the effective floor thickness ($=\beta g\Delta T H^3/\nu^2$). Fig. 7 shows the variation of the coefficient of discharge with the Grashof number for both opening configurations. This dependency was found to conform to the following relationship:

$$C = 11.85Gr_H^{-0.2} \tag{13}$$

The coefficient of discharge and the Grashof number were correlated very well with r^2 value equal to 0.96 (Fig. 7).

4. Numerical simulations

4.1. CFD algorithms

The computational fluid dynamics (CFD) method was used to simulate the cases corresponding to the eleven experiments described in the previous section. It must be noted that buoyancy driven flows are difficult to model using CFD techniques. The main reasons are as follows: small driving forces can lead to numerical instabilities; selection of the most accurate turbulence model determines the final predictions; the flow is implicitly specified since it is induced by thermal buoyancy; the definition of boundary conditions is not usually accurate and complete. However, a series of simulations were carried out in order to investigate the ability of this method to model these phenomena. These simulations were performed, applying CFD al-

gorithms which have recently developed in University of Athens. The adopted algorithms have been validated through comparative simulations against the well established commercial tool of PHOENICS [16]. In particular, a number of cases concerning air flow around obstacles and air flow in the interior of enclosures, were selected. Then each case was simulated by using the specific algorithms and subsequently by applying PHOENICS, ensuring that the computational characteristics, the grid size, the inclusion of turbulence model and the boundary conditions were alike for both simulations. Comparison between the corresponding predictions of air velocity, temperature and concentration level distribution showed very good agreement.

These algorithms generate approximate solutions to the Navier-Stokes equations, which are considered universally valid to describe the flow of a fluid, heat and concentration in a specific field. These equations are based on the conservation equations of mass, momentum, energy (enthalpy) and concentration species. Since Rayleigh numbers based on the height of the whole experimental space, were found to range from 2 $\times 10^{10}$ to 1×10^{12} during all the experiments, turbulence calculations were included. It must be noted that turbulence modeling is a crucial aspect of CFD methods, but is particularly important in buoyancy-driven flows in which the buoyancy forces increase turbulent activity. To numerically simulate this turbulence, this study used the more recent RNG k–ϵ model based on the Renormilized Group theory established by Yakhot *et al.* [17]. In this model the constants appearing in the transport equations for kinetic energy and energy dissipation rate are derived mathematically and not empirically as in other turbulence models. The advantage of this derivation is that this model is valid for a very wide range of flow types including both high and low Reynolds number flows.

4.2. Solution procedure

The governing equations were spatially descretized over a staggered grid using the finite volume method, based on a Cartesian grid. The power-law differencing which gives physically realistic solutions even for coarse grids was used for the convective-diffusive

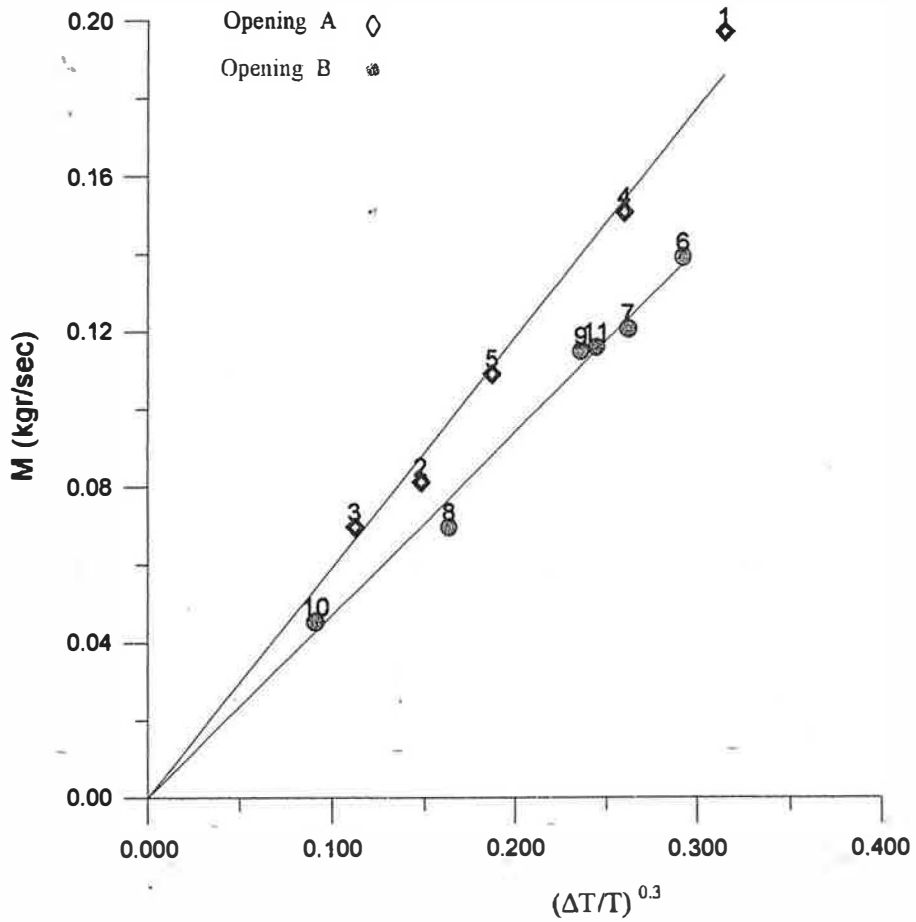

Fig. 6. Mass flow rate vs $(\Delta T/T)^{0.3}$ for both opening sizes (◇, ●: run, – – –: Eq. (11)).

fluxes. The source terms were linearized. The pressure and velocities were coupled using the SIMPLE algorithm developed by Patankar [18]. These equations were solved numerically using the line-by-line procedure and the Tri-Diagonal Matrix Algorithm (TDMA). Computations were time-dependent to deal with the concentration decay and the highly transient flow field. The fully implicit scheme was adopted. This scheme does not dictate any restrictions on the time-interval selection, as other schemes do, and satisfies generally the common requirements for simplicity and physical behavior. Small time steps of around 1/10 of the characteristic time scale were used in order to improve the accuracy of the results. The characteristic time scale for each run was considered as the time required to achieve uniformity concerning the concentration level throughout the whole experimental space. The computations were performed over the whole period of each experiment.

Computations were also three-dimensional since the flow had been expected to be highly asymmetrical due to the complex geometry of the building. For simplicity, an orthogonal, equally spaced grid system was used to cover the domain. Concerning the stairways, a simplified geometry was adopted. In particular, it was assumed that the individual steps were orthogonal blocks, as opposed to being smooth on the underside, and based on this assumption an orthogonal grid was used in the vicinity of the stairs. Five different grid sizes were investigated to determine the necessary resolution for grid-independent solutions. These grid sizes ranged from 2160 cells ($15 \times 9 \times 16$) to 35,280 cells ($42 \times 20 \times 42$). Comparison of simulated volumetric flow rate through the opening separating the two zones, showed that a grid-independent solution was achieved by using a $30 \times 14 \times 30$ mesh (12,600 cells). Since the main objective was to model the general flow patterns and to predict the volumetric air flow rate between the zones, further refinement of the grid would not produce any appreciable gains in accuracy. The main criterion for convergence was to achieve a small value ($\sim 10^{-4}$ kg s^{-1}) for the sum of the mass residuals at the end of each time step. However, the convergence becomes quite problematic in low-Reynolds number flows. Therefore, tight control was required in the solution process. Variable under-relaxation factors for velocity components were applied during simulations in order to achieve convergence.

The boundary conditions and the initial conditions were carefully set for each zone. Surface temperatures were different for individual cases. Furthermore, at the beginning of each test, the upper and lower zone had different uniform air temperatures and concentration levels. These necessary values were provided by the measurements during the experiments. In addition, a small opening was built into one of the side walls of the upper zone and the building was otherwise airtight.

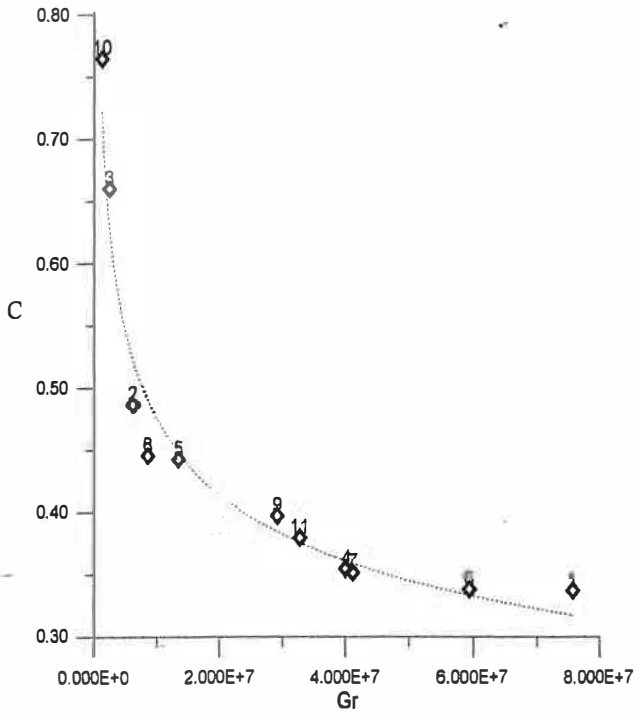

Fig. 7. Variation of coefficient of discharge C with the Grashof number (◇: run, – – –: Eq. (13)).

4.3. Results and discussion

During these transient simulations, mass and energy transfer between the two zones caused variations in air temperature and velocity. These were recorded and analyzed to reveal air flow patterns, temperature differences, air flow rates and their variation with time. The volumetric air flow rate between the two zones is calculated using:

$$Q = \sum_{i=1}^{n} | Wi | Ai/2 \tag{14}$$

where n is the number of cells within the span of the horizontal opening of the stairwell, W_i is the vertical component of air velocity at individual grid points within the opening and A_i is the area perpendicular to $W1_i$ of individual cells within the opening. These rates were calculated at the end of each time step. Then they were averaged over the whole duration of each experiment. The final values were compared with experimental measurements, presented in Table 2. The absolute value of the relative difference between the simulated predictions and experimental measurements ranged from about 1.2 to 11.6%, with an average value equal to 5.5% for all the experiments. Fig. 8 shows these results. This is a very good agreement, considering the

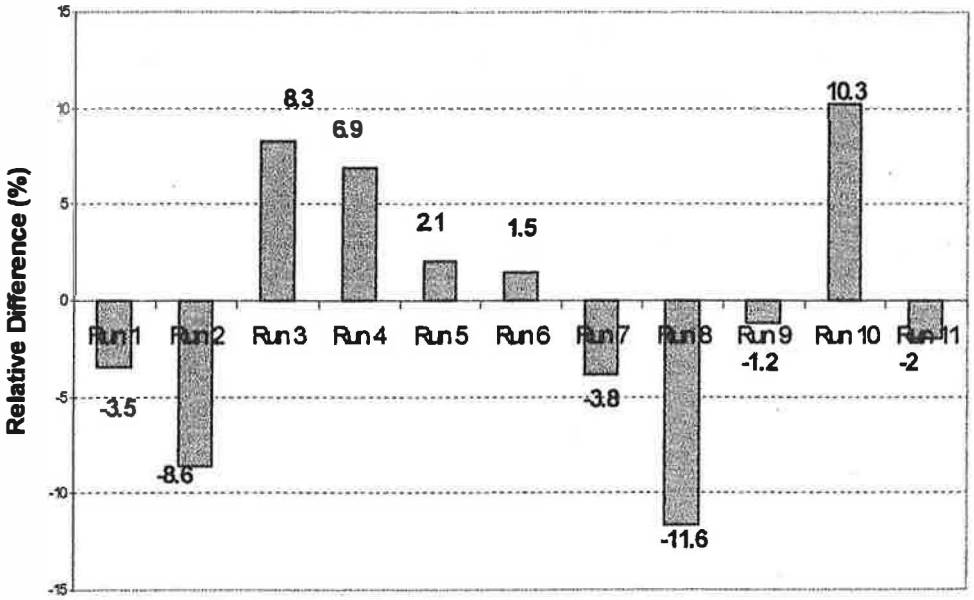

Fig. 8. Relative differences between the measured and simulated volumetric air flow rate through the stairwell.

many factors — such as the turbulence model, experimental errors and boundary conditions — which affect the accuracy of the results.

The analysis of these predictions also revealed the general features of the flow in the zones, as well as in the opening separating the two zones. Figs. 9 and 10

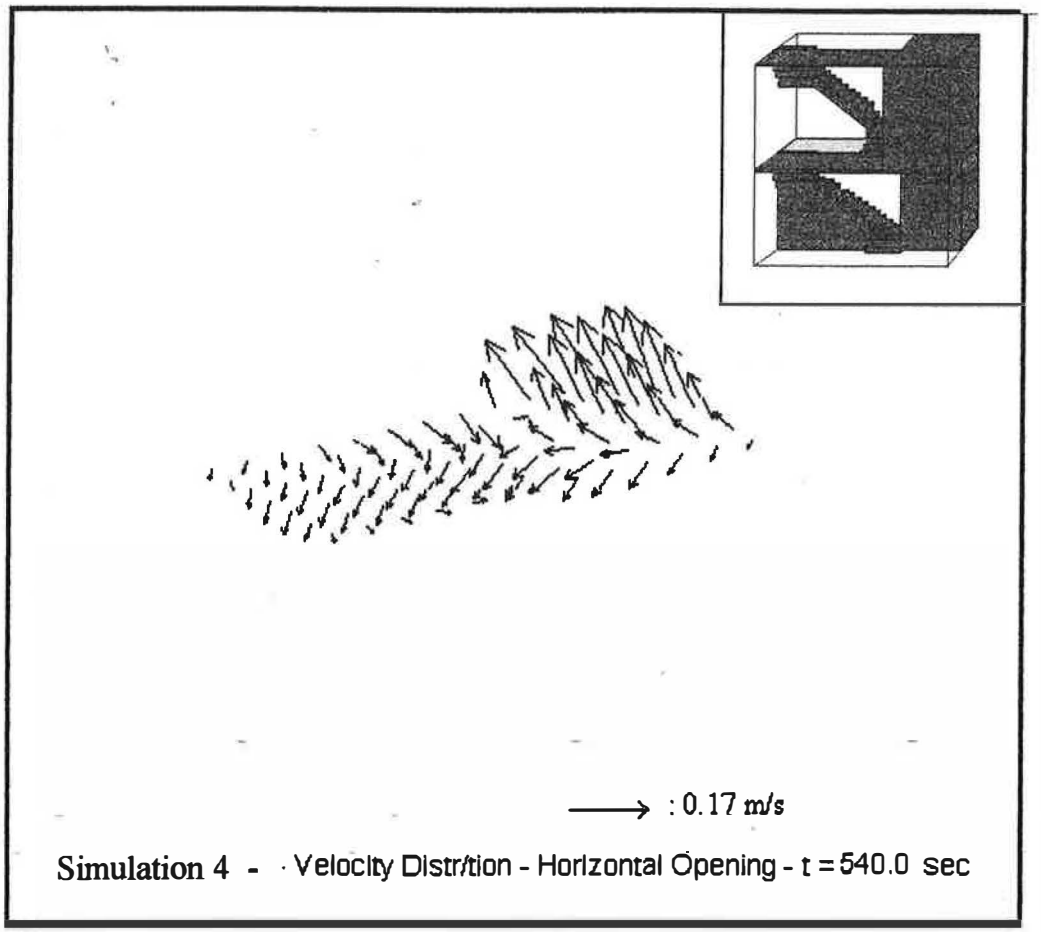

Fig. 9. CFD simulation of flow pattern within the opening of the stairwell at $t = 540$ s during the simulation corresponding to the fourth run.

show typical flow patterns obtained from these simulations, in the opening and in the two zones respectively, at a moment 540 s into the computer simulation corresponding to the fourth experiment. The arrows indicate the flow directions and flow velocities by using stems with lengths proportional to the local air speed. It was found that these patterns were affected mainly by the stairwell geometry and the temperature difference between the zones. The simulations revealed a warm upflow over a cold downflow along the stairs. This counterflow affected the flow pattern in the horizontal opening. Indeed, warmer air from the lower zone was rising through the front part of the opening into the upper zone while cooler air moving downward through the remainder of the opening, except in the region close to the floor where the effect of descending cooler air was dominant (Fig. 9). The extent of the part corresponding to the cooler descending air stream was greater than the other corresponding to the warmer rising air stream. Since there was no net flow, the velocities of warmer air were greater than the velocities of the cooler air. This pattern was mainly attributed to the presence of stairs just below the part of the opening corresponding to the cooler descending air flow. This flow pattern did not change significantly with time. As a result, the stairwell geometry seemed to form a relatively stable velocity distribution along the opening. On the contrary, other studies concerned with the air flow through independent horizontal openings, indicated that the flow pattern was highly transient and varied considerably with time [9]. This steady behavior of the flow observed in the present work was caused by the influence of the specific stairwell geometry. However, when the average temperature difference between the zones decreased, the flow through the opening became weaker and the corresponding flow pattern less steady with time. This flow pattern agreed generally with the flow visualization tests. Concerning the flow pattern in the zones, the lower zone was dominated by many vortices, which promoted heat transfer and uniformity of temperature and concentration level within the zone (Fig. 10). A similar situation was found in the upper zone. The higher the temperature difference, the more intense the eddies. Furthermore, the three-dimensional behaviour of the flow was found to be strong due to the complex geo-

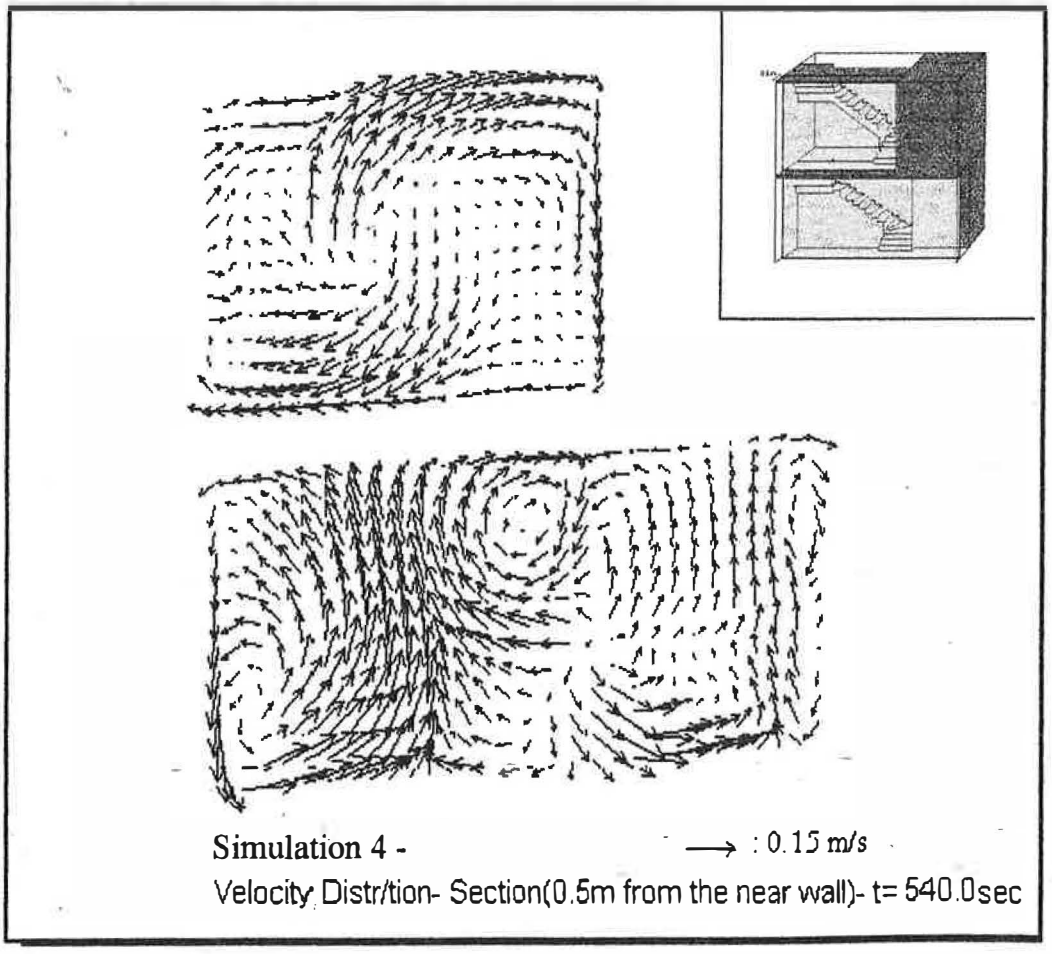

Fig. 10. CFD simulation of flow pattern within the two zones at t = 540 s during the simulation corresponding to the fourth run.

metry. The flow pattern was markedly different close to the side walls. Here the air was moving downwards along these walls, an effect which was enhanced as a consequence of the heat loss to the wall, except in the region close to the left side wall of the upper zone where the effect of the warm rising air was quite strong. The transient simulations indicated that these flow patterns experienced relatively small variations with time.

The simulations also predicted the air temperature and concentration level distribution in both zones for all the cases. The predictions of these variables indicated the homogeneity observed by the measurements to characterize each zone. Comparison between the measured and the predicted air temperature for each zone showed very good agreement. Particularly, the absolute value of the mean differences between the measured mean air temperature and the corresponding simulated one for both zones was found to range from about 0.2 to 0.6°C for all cases. Similarly, comparison between the measured and the predicted concentration level for each zone showed encouraging agreement. The absolute value of the relative difference between the measured mean concentration level and the corresponding predicted one for both zones was found to be less than 17.5% for each time step and each experiment. Furthermore, the absolute value of the mean relative differences between measured and simulated values, for all the time steps of each experiment, were even lower. These results are presented in Fig. 11. The total mean value of the absolute values of the relative differences was 8% or 0.08 for the lower zone and 9% or 0.09 for the upper zone. It must be noted that these predictions were found to overestimate the concentration level for almost all the comparisons with the experimental data. This overestimation can be attributed to the presence of infiltration/exfiltration during the measurements, which is particularly very difficult to model using CFD methods. However, these simulations showed generally good agreement with experiments for two main reasons: the infiltration rate was found to be quite low, as already mentioned and the duration of experiments was relatively small. These reasons justified that the exclusion of the infiltration process from the simulations did not affect significantly the reliability of the predictions.

5. Conclusions and recommendations

Buoyancy-driven flows within the rather complex geometry of a stairwell of a full-scale building were studied experimentally, analytically and numerically. The application of the single tracer gas technique was found to be a convenient method for estimating inter-zone air flows, although, the accuracy of measurements could be improved by using multiple tracer gas techniques. The measurements indicated the homogeneity characterizing each floor during the experimental stage. In conclusion, all floors connected by a stairwell proved to behave as different zones, at least for the relatively small exchange rates of density-driven flows.

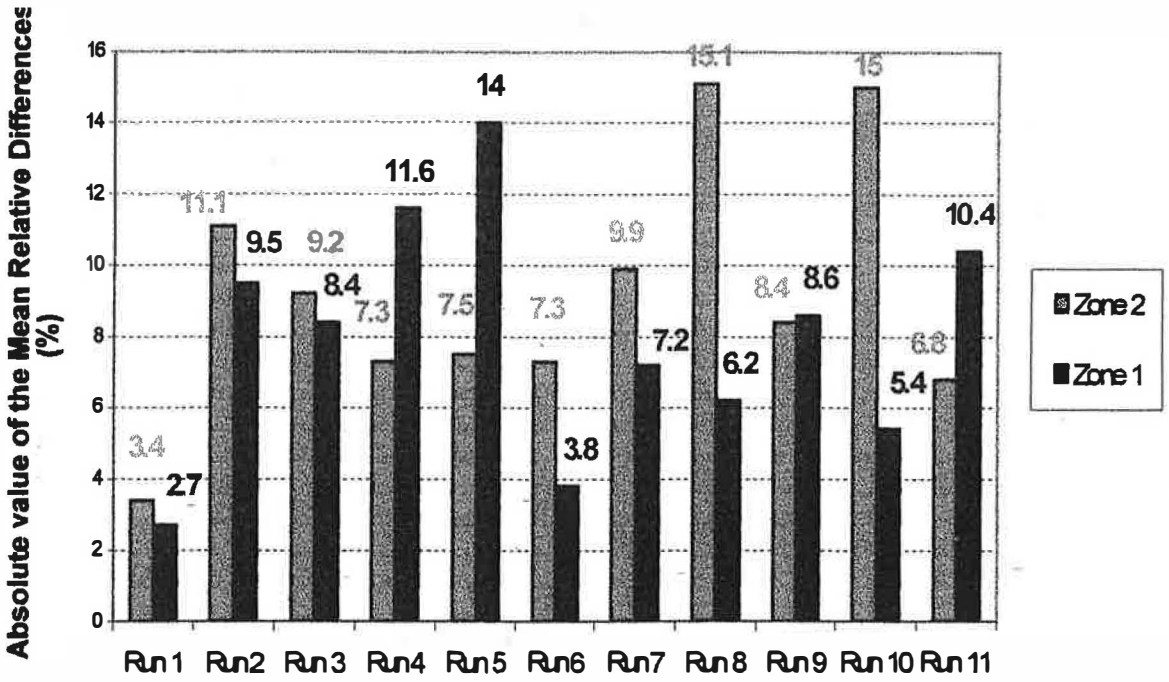

Fig. 11. Absolute value of the mean relative differences between the measured and simulated N_2O concentration level for all the runs.

The theoretical approach of air flow through a horizontal opening formed by the stairwell geometry was adopted for the derivation of mass and heat flow rate between the floors. The experimental results showed that the coefficient of discharge characterizing the flow through the opening appeared to be dependent only on the average temperature difference between the zones and not on the size of this opening. However, this result cannot be generalized since only two opening sizes were investigated in this study. The coefficient of discharge was found to decrease as the interzone temperature difference increased. This decrease was attributed to an increase of interfacial mixing between the warmer rising flow and the cooler descending flow and to an increase in turbulence as the temperature difference increased. Further experimental work is required to investigate the possible effects of stairwell geometry and size of the opening on the value of this coefficient.

The volumetric flow rate through the opening connecting the two zones was found to be a function of the interzone average temperature difference and size of this opening. The mass and heat flow rate through the opening were also found to be functions of the interzone average temperature difference and size of the opening. These rates increased significantly with increasing temperature difference. In particular, the mass and heat flow rate increased linearly with $(\Delta T/T)^{0.3}$ and $(\Delta T)^{1.3}/T^{0.3}$, respectively. These rates also appeared to increase linearly with A, the effective area of the opening and $(H)^{0.5}$, the square root of the effective thickness of the floor separating the two zones. It is a matter for further experimental work to discover the applicability of these correlations for the estimation of mass and heat transfer between floors in buildings with more than two floors and, in addition, to investigate whether these correlations vary markedly from one stairwell type to the next and possibly to establish generalized equations for the more common stairwell forms.

CFD three-dimensional transient simulations of these cases were carried out. Comparison between the simulated volumetric airflow rates between the zones and those based on experimental measurements showed very good agreement, with an absolute value of the relative difference remained below 11.6%. Furthermore, comparison between the simulated air temperature and concentration level field and those based on measurements revealed encouraging agreement, despite the difficulties of the CFD method to model these processes. These computations revealed also the overall features of the flow. The relatively stable velocity distribution in the region within the horizontal opening connecting the two zones can be attributed to the specific stairwell geometry. This particular geometry produced a strong three-dimensional flow in each zone, dominated by many vortices which prevent thermal isolation of these zones. Further investigation is required to improve the effectiveness of these algorithms to model these air flow phenomena.

References

[1] Brown WG. Natural convection through rectangular openings in partitions-2: horizontal partitions. Int J Heat and Mass Transfer 1962;5:869–81.

[2] Epstein M. Buoyancy-driven exchange flow through small openings in horizontal partitions. Trans of the ASME, Journal of Heat Transfer 1988;110:885–92.

[3] Klobut K, Siren K. Air flows measured in large openings in a horizontal partition. Building and Environment 1994;29(3):325–35.

[4] Reynolds AJ. The scaling of flows of energy and mass through stairwells. Building and Environment 1986;21(No 314):149–53.

[5] Zohrabian AS, Mokhtarzadeh MR, Reynolds AJ, Marriott BST. An experimental study of buoyancy-driven flow in a half scale stairwell model. Building and Environment 1989;24:141–8.

[6] Reynolds AJ, Mokhtarzadeh-Dehghan MR. The modeling of stairwell flows. Building and Environment 1988;23(No 1):63–6.

[7] Riffat SB. Measurement of heat and mass transfer between the lower and upper floors of a house. Int J of Energy Research 1989;13:231–41.

[8] Ergin-Ozkan S, Mokhtarzadeh MR, Reynolds AJ. Two- and three-dimensional finite volume predictions of flow in a stairwell and comparison with experiment. In: Proceedings of International Symposium on Room Air Convection and Ventilation Effectiveness, University of Tokyo, 1992. p. 201–6.

[9] Riffat SB, Shao L. Characteristics of buoyancy-driven interzonal airflow via horizontal openings. Build Serv Eng Res Technol 1995;16(3):149–52.

[10] Feustel H, Zuercher Ch, Diamond R, Dickinson B, Grimsrud D, Lipschutz R. Temperature- and wind-induced air flow patterns in a staircase: Computer modelling and experimental verification. Energy and Buildings 1985;8:105–22.

[11] Edwards R, Irwin C. Two-directional air movements in stairwells. In: Proceedings of 11th AIVC Conference, Belgirate, Italy. vol. 21. p. 379–88.

[12] Okuyama H. System identification theory of the thermal network model and an application for multi-chamber airflow measurement. Building and Environment 1990;25(4):349–63.

[13] Sinden FW. Multi-chamber theory of air infiltration. Building and Environment 1978;13:21–8.

[14] Afonso CFA, Maldonado EAB. Single tracer gas method to characterize multi-room air exchange. Building and Environment 1986;9(4):273–80.

[15] Roulet CA, Vandaele L. Airflow patterns within buildings — measurement techniques. Annex 20, IEA, 1991.

[16] Spalding DB. The PHOENICS encyclopedia. London: CHAM Ltd, 1994.

[17] Yakhot V, Orszag SA, Thangham S, Gatski TB, Speziale CG. Development of turbulence models for shear flows by a double expansion technique. Phys Fluids A 1992;4(7):1510–20.

[18] Patankar SV. Numerical heat transfer and fluid flow. NY: Hemisphere, 1980.